TRANSFER TRAJECTORY OPTIONS FOR SERVICING SUN-EARTH-MOON LIBRATION POINT MISSIONS

David C. Folta* and Cassandra Webster[1]

Future missions to the Sun-Earth Libration L_1 and L_2 regions will require scheduled servicing to maintain hardware and replenish consumables. While there have been statements made by various NASA programs regarding servicing of vehicles at these locations or in Cis-lunar space, a practical transfer study has not been extensively investigated in an operational fashion to determine the impacts of navigation and maneuver errors. This investigation uses dynamical systems and operational models to design transfer trajectories between the Sun-Earth Libration region (QuasiHalo orbit) and the Earth-Moon vicinity (Distant Retrograde Orbit, QuasiHalo Orbit, Halo Orbit, and Near Rectilinear Halo Orbit). We address the total ΔV cost of transfers and operational considerations between each pair of locations using a Monte Carlo analysis.

INTRODUCTION

Future missions to the Sun-Earth Libration L_1 and L_2 regions will require scheduled servicing to maintain hardware and replenish consumables. While there have been statements made by various NASA programs regarding servicing of vehicles at these locations or in Cis-lunar space, a feasibility study of transferring these vehicles has not been extensively investigated in an operational fashion. [1,2,3,4] The design of the related transfer trajectories between locations are dependent on orbit types and their dynamical system properties, departure and arrival conditions, and the servicing vehicle's capabilities. Sun Earth-Moon Libration science missions will accommodate multiple orbit types, from large QuasiHalo to smaller Lissajous. Initial orbit conditions considered here are based on upcoming missions such as the Wide-Field Infrared Survey Telescope (WFIRST). The servicing vehicle is assumed to be in the Earth-Moon vicinity and this investigation provides trajectory designs of transferring the servicing vehicle from the Earth-Moon region or proposed Gateway orbit to the Sun-Earth L_2 (SEL_2) region, and transferring the mission spacecraft from SEL_2 back to the Earth-Moon vicinity.

The analysis done in this paper begins with a dynamical systems approach as an initial strategy. Then using numerical computation with high fidelity models and linear and non-linear targeting techniques, the various maneuvers and ΔV's associated with each orbit and related transfer are computed. From a dynamical system standpoint, we speak to the nature of these orbits and their stability. The existence of a connection between unstable regions, such as manifolds between the Earth-Moon and Sun-Earth Libration point systems, enables mission designers to envision

---

* Senior Fellow, Aerospace Engineer, NASA Goddard Space Flight Center, Greenbelt, MD, 20771, david.c.folta@nasa.gov

[1] WFIRST Flight Dynamics Lead, NASA Goddard Space Flight Center, Greenbelt, MD, 20771, cassandra.webster@nasa.gov

.

scenarios of multiple spacecraft traveling economically from system to system, rendezvousing, servicing, and refueling along the way. We address the cost of transfers between each pair of locations. Early analysis suggests these transfer ΔV costs can range from centimeters per second for the more unstable orbits to nearly tens or possibly hundreds of meters per second for the stable co-linear locations.[5,6] Of course ΔV cost depends on several parameters, such as orbit amplitudes (as measured in a rotating, libration centered coordinate system), mis-modeled accelerations due to solar radiation pressure and third body gravity, the calibration of the propulsion system, and the accuracy of the navigation solutions. Additionally, the location in the respective orbits and overall timing play a major role in being able to establish these transfers. Our analysis incorporates these errors and timing considerations in non-linear control efforts to estimate the transfer cost.

To determine feasible designs across various dynamical regions, several tools are employed which are grounded in the dynamical properties of the science orbits and maintenance regions as well as the dynamics of their transfers. These tools include the Goddard and Purdue developed software tool, Adaptive Trajectory Design (ATD), used to model dynamical systems and to represent natural transfer manifolds, and AGI's STK® software to design transfers in a high fidelity environment. The results of this paper provide an assessment of possible transfers, highlighting the total ΔV due to navigation and maneuver uncertainties, their transfer durations, orbit geometry influences, and other trajectory parameters of interest.

EARTH-MOON AND SUN-EARTH ORBIT EXAMPLES

For this study, the servicing vehicle is assumed to be in the Earth-Moon vicinity and the orbits that are considered in this analysis include a planar Lunar Distant Retrograde Orbit (DRO), Earth-Moon L_2 Halo and QuasiHalo orbits, and the proposed Lunar Gateway Near Rectilinear Halo Orbit (NRHO). Earth-Moon L_1 orbits were not included in this study because transfers between Earth-Moon L_2 (EML$_2$) and Earth-Moon L_1 have been operationally demonstrated in 2012 by the Acceleration, Reconnection, Turbulence and Electrodynamics of the Moon's Interaction with the Sun (ARTEMIS) mission. [7] Current considerations for servicing are focused only on the above orbit types due to assumptions of ΔV cost and transfer trajectory requirements.

Figures 1 through 5 present the orbits used in this analysis and Table 1 presents the Cartesian components in their respective coordinate frames and dynamical systems parameters for each orbit. The Jacobi Constant (JC) is measured in the respective orbit system, e.g. SEL$_2$ or EML$_2$ and the stability index (SI) is the stability of the system and indicates the need for stationkeeping as well as the ease of departure from or insertion into these orbits. As the SI approaches a value of '1', the orbit becomes more stable. While this is a benefit for stationkeeping, it also means that the ΔV required to depart will increase. Figures 1 through 3 show the Earth-Moon orbits (NHRO, DRO, Halo, and QuasiHalo) while Figure 4 shows the principal WFIRST SEL$_2$ QuasiHalo orbit design used for this analysis. The Earth-Moon L_2 Halo orbit shown was constructed to represent a minimum shadow orbit and, in this case, provides shadow free orbits for more than a year at a time. The EML$_2$ QuasiHalo and DRO are of the Lyapunov type to compare to Halos which have an out-of-plane component resulting in additional departure or insertion constraints and ΔVs for alignment of the transfer to or from SEL$_2$. Lastly, a NRHO was simulated based on the proposed Gateway orbit.[8] All orbits were generated using an initial epoch date of January 1st, 2030. This date was chosen to reflect the possible timeline of such servicing missions and provides feasible launch opportunities for the transfers to and from the servicing regions.

In a concluding section, we discuss the transfer design differences starting from the above Earth-moon locations to either the principal WFIRST QuasiHalo orbit or to a large SEL$_2$ Lissajous orbit which is also deigned to meet WFIRST orbit requirements. This comparison provides a basis

for the transfer cost and insertion cost into both orbit types and allows one to determine if the correction maneuvers are similar.

Table 1. Orbit Parameters, Maximum Values

Orbit	X Amplitude (km)	Y Amplitude (km)	Z Amplitude (km)	SI* U/S	JC*	Comment	Approx Orbit Period (day)
EML$_2$ Halo	-14608	37246	-11382	1172	3.2	Minimum Shadow	15 (EML$_2$)
EML$_2$ QuasiHalo	-21618	46212	0	947	3.1	ARTEMIS type	15 (EML$_2$)
Lunar DRO	-132353	-91663	0	1	2.9	Small amplitude DRO	13 (moon)
NRHO (Gateway)	-67133	17216	-70051	1.5	3.0	Gateway design	7.2 (moon)
QuasiHalo SEL$_2$ (WFIRST)	-281891	721222	-244395	1536	3.0	WFIRST selected orbit	180 (SEL$_2$)
Lissajous SEL$_2$	206887	542200	444011	1500	3.0	Shadow Free design	180 (SEL$_2$)

*Approximate values based on ATD constructed orbits

Initial Transfer Designs

Once the proposed servicing vicinity and prime mission orbits were selected, the task then turned to the initial design of the transfer orbits. The transfers considered here are designed to minimize (not optimize) the total ΔV and transfer duration by using the natural dynamics in the Earth-Moon and Sun-Earth regions. The idea behind this process was to rely on the natural motion and the software tools developed over the last several years to construct such orbits. The initial transfers that provide the guidance on where to place departure and arrival maneuvers are based on dynamical systems within the ATD tool [9] to find the natural trajectories to transfer between the two regions of interest.
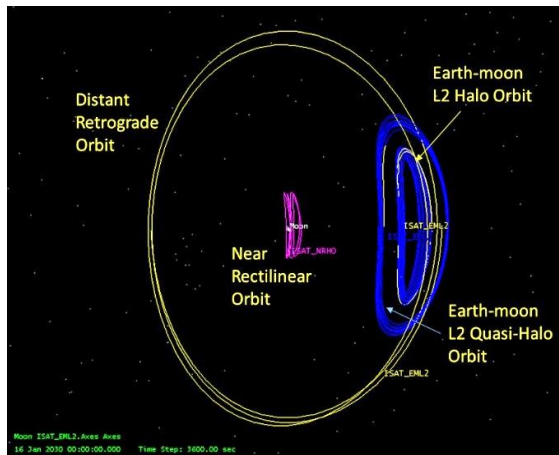

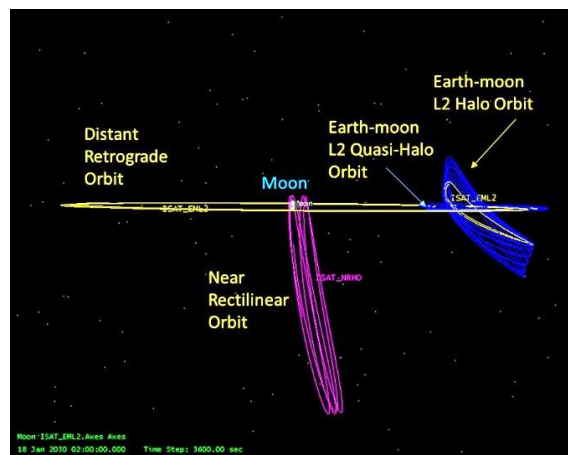**Figure 1. Halo, QuasiHalo, DRO, and NRHO in Rotating Coordinates, view from EML$_2$ +Z axis**

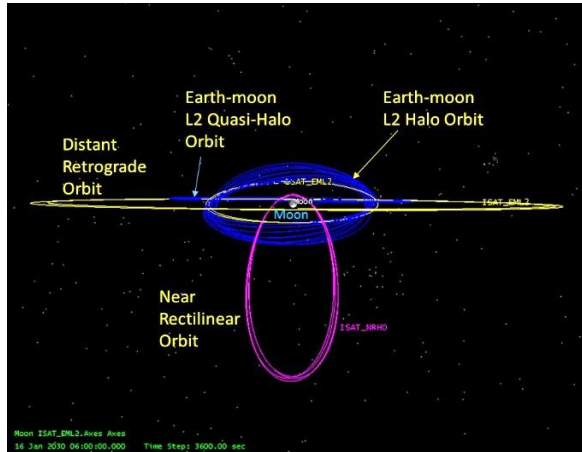**Figure 2. Halo, QuasiHalo, DRO, and NRHO in Rotating Coordinates, view from EML$_2$ -Y axis**

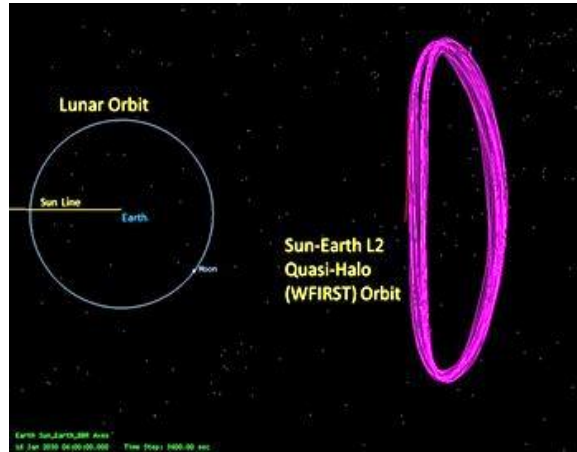**Figure 3. Halo, QuasiHalo, DRO and NRHO in Rotating Coordinates, view from EML$_2$ +X axis**

Figure 4. WFIRST SEL$_2$ Orbit, in Rotating Coordinates, view from SEL$_2$ +Z axis

ATD is an original and unique concept for quick and efficient end-to-end trajectory designs using proven piecewise dynamical methods. ATD provides mission design capabilities of cis-lunar, Earth-Moon, and Sun-Earth orbits within unstable/stable regions through the unification of individual trajectories from different dynamical regimes. Based on a graphical user interface, ATD provides access to solutions that exist within the framework of the Circular Restricted Three Body Problem in order to facilitate trajectory design in an interactive and automated way. ATD was developed under the Fiscal Year 2012 and 2013 NASA GSFC Innovative Research and Development programs.

Other mission design approaches using commercial and NASA software tools, such as AGI's STK/Astrogator ® and Goddard's open source General Mission Analysis Tool (GMAT), complete each trajectory design phase in isolation with the beginning/end state information from one regime used to kick-off the design process in the next regime. Such a serial design strategy can be time-consuming and yields a result with the possibility that the optimal combination is overlooked. In contrast, ATD allows disconnected arcs to be conceptually devised in different frames (inertial, rotating, libration point) and models (conic, restricted three-body, ephemeris). Then the individual arcs are blended to leverage the advantages of each dynamical environment. The ARTEMIS mission was supported by GSFC in this manner since each section/phase of the trajectory, i.e., near Earth, Sun-Earth, and Earth-Moon, was required to be part of a continuous trajectory flow. Current design processes are not automated and, once a continuous solution exists, it is not possible to substantially modify the overall design without a new start and a significant time investment. ATD provides access to a composite view of multi-body orbits possessing a variety of characteristics within an interactive design setting. The availability of a large assortment of orbit types within one mission design environment offers the user a unique perspective in which various mission design options may be explored, and the effectiveness of different orbits in meeting mission requirements may be evaluated. Once a discontinuous baseline is assembled within the design environment, it is then transitioned into a unified higher-fidelity ephemeris model via interactive ATD differential correction environments. The final trajectory for this analysis was used as the initial guess in simulations using AGI's Astrogator module in STK.

The initial transfer manifolds between the Earth-Moon orbits and the SEL$_2$ WFIRST orbit are shown in Figures 5 through 8. These ATD generated manifolds show numerous possible transfers, from which we down-selected transfers that would arrive at asymptotes that were advantageous to lower ΔV cost, that is, at an angle that represented approaches that are tangential to the orbit of

interest and along the local stable or unstable EML$_2$ manifold. Figure 7 shows all the unstable manifold transfer trajectories between the WFIRST orbit and reaching the lunar orbit radius. It is obvious from this plot that while numerous transfers exists, a smaller family provides a lower angle at arrival. Figure 6 shows the stable manifolds for transfers from the Earth-Moon region to SEL$_2$. Figure 7 and 8 show the transfers which provide lower approach or departure angles, and were chosen to be less than a $30°$ angle between the lunar orbit and the incoming or outgoing transfer to SEL$_2$. The defined 'flightpath' angle is the angle between the manifold arc velocity vector in the rotating frame and the vector tangent to the lunar radius circle at the location where the manifold arc reaches the lunar radius. The data in Figures 7 and 8 are symmetric with the stable and unstable manifolds mirroring each other over the $y = 0$ plane. The green manifolds in Figures 7 and 8 are the stable (outgoing) manifolds from the Earth-Moon system while the pink are the unstable manifolds into the Earth-Moon system.
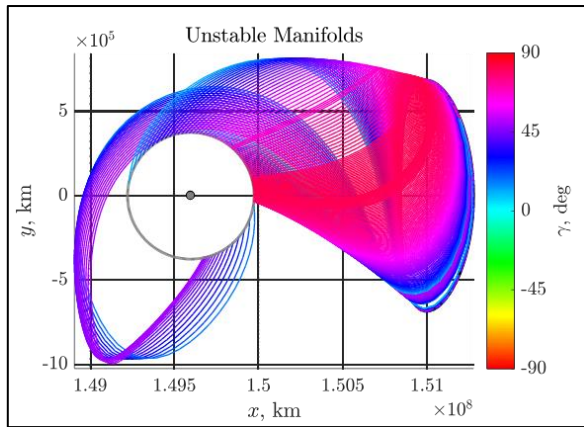

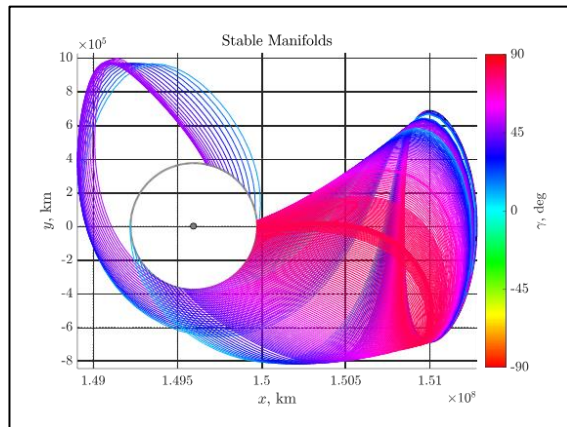**Figure 5. UnStable Manifold Transfer from SEL$_2$ to Lunar Orbit**

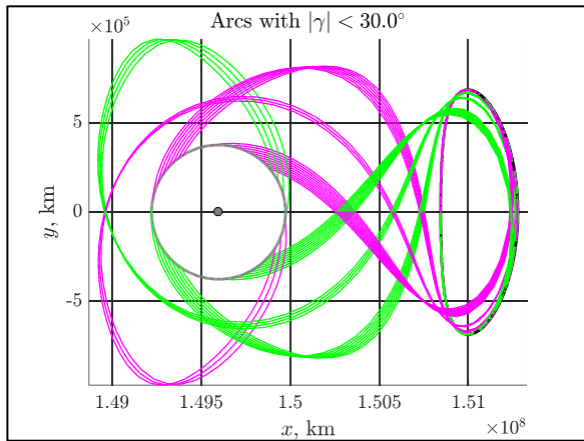**Figure 6. Stable Manifold Transfers from Lunar Orbit to SEL$_2$**

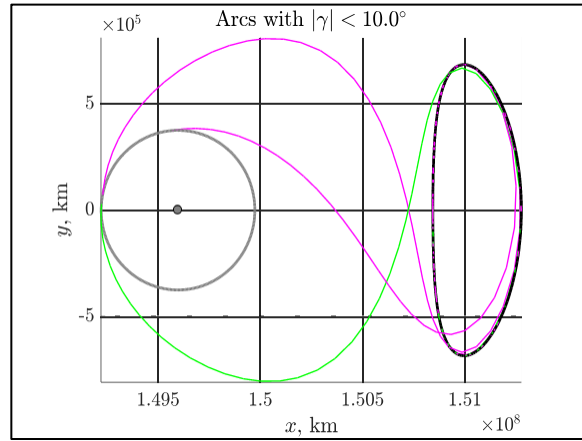**Figure 7. Stable and Unstable Manifold Transfer between SEL$_2$ to Lunar Orbit, Angle <30°**

Figure 8. Stable and Unstable Manifold Transfer between SEL$_2$ to Lunar Orbit, Angle

In addition to these transfers between the Earth-Moon and SEL$_2$ orbits, we also looked at the flows emanating from the example Earth-Moon orbits in question. Again, ATD was used to determine and plot the lunar local manifolds similar to the SEL$_2$ transfers. The reason was to determine a general location for the departure or arrival maneuver, and to minimize that ΔV. Figures 9 and 10 present the stable and unstable flows with respect to the QuasiHalo orbit and Figures 11 and 12 present similar flow information for the EML$_2$ Halo orbit. The arrows indicate

the direction of motion. The DRO and NRHO orbits will not have a local manifold as the SI is lower and the manifold would take numerous revolutions to depart.
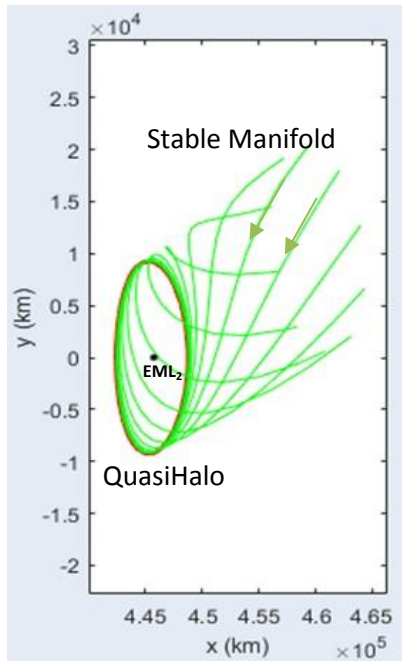

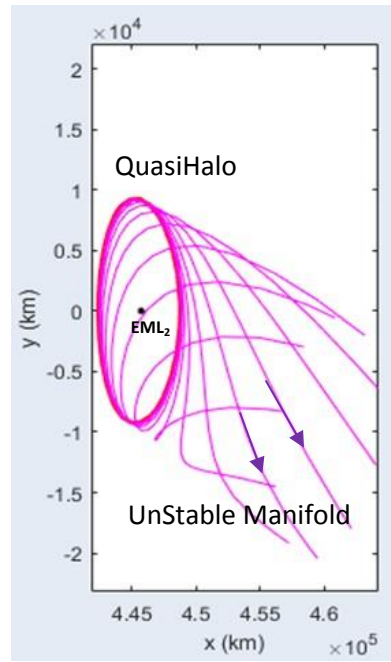**Figure 9. Stable (approach) Manifold to EML₂ QuasiHalo Orbit**

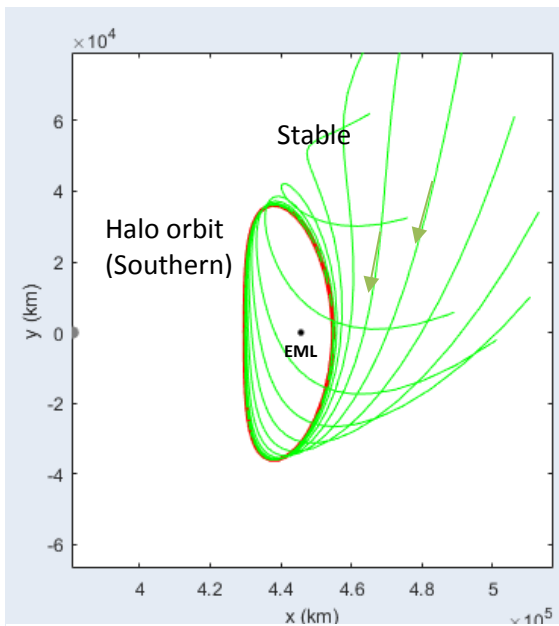**Figure 10. UnStable (Departure) Manifold from EML₂ QuasiHalo Orbit**

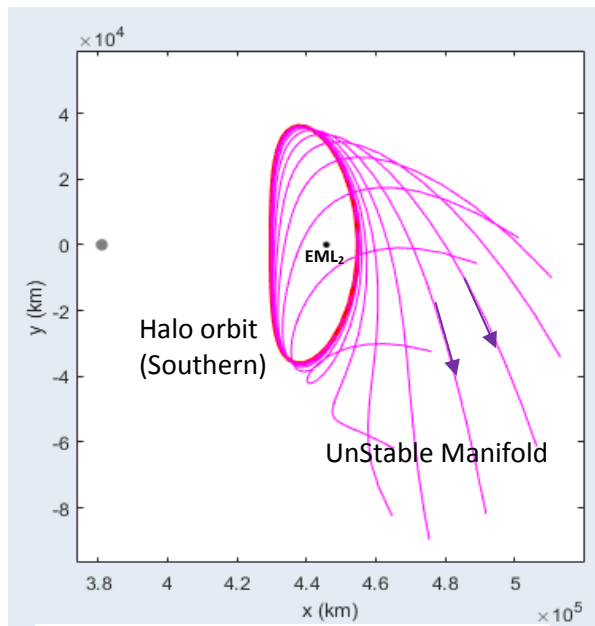**Figure 11. Stable (approach) Manifold to EML₂ Orbit**

Figure 12. UnStable (Departure) Manifold from EML₂ Orbit

Initial High Fidelity Transfer Generation

As shown in the above ATD transfers, we reduced the arrival flight path angle to represent lower ΔV cases such that trajectories do not intersect with the required arrival or departure orbit at an acute angle. Following the transfers shown in Figures 7 and 8 with flightpath angles $< 30°$, it can be seen that the departure and arrival conditions are limited to the far side of the SEL$_2$ WFIRST orbit for either departure or arrival. The departures and arrivals near the Moon are constrained to Sun-Earth-Moon angles near $120°$ and $50°$. This consequence has been common knowledge for mission designers using a dynamical systems application. [10,11]

A higher fidelity modeling was then used to match the orbits selected for analysis with the ATD advised manifolds. This modeling was done to design reference transfers that included the ΔVs for departure and arrival.

The WFIRST Reference Orbit

The WFIRST orbit is used as a 'reference' orbit for this analysis as its orbit and spacecraft design includes the possibility of servicing. WFIRST will launch in 2025 and will be placed into a QuasiHalo SEL$_2$ orbit. **This orbit** size meets future observatory requirements as well. The orbit has a smaller SEL$_2$ Y-amplitude than JWST, but can be considered a reasonable size. The orientation of the SEL$_2$ orbit, as seen in upcoming figures, can drive ΔV requirements for servicing. The orbit is modeled using the baseline WFIRST design. [12] Additionally, for comparison of EM libration orbit to SEL$_2$ ΔVs, a Lissajous orbit was constructed to meet the WFIRST requirement of no Earth shadow and to achieve a minimal S/C-Sun-Earth angle of three degrees.

SEL$_2$ to EML$_2$ Halo, QuasiHalo, DRO and NRHO transfers

To ensure that the transfer design from SEL$_2$ to the Earth-Moon region would close, we used an inverse integration approach where we started the process with the orbit to be inserted into as the 'initial condition' and then propagated **in reverse** and used a differential corrector (DC) targeting approach to finalize the completed transfer. Once that **reverse** design was converged upon, a forward propagated DC approach reproduced the design, but starting with the end condition of the reverse analysis. This forward simulation provides the basis of the Monte Carlo analysis that includes navigation and maneuver errors in an operational scenario to determine the total ΔVs to transfer a spacecraft between SEL$_2$ and the EML$_2$, DRO, or NRHO orbits.

A single transfer for each case was designed although several transfers were investigated to determine the variation in the ΔVs. It was expected that the departure and arrival ΔVs would be a function of their placement on the orbits. This was found to be the case and a reasonable ΔV was chosen for each as a representative design. Given that operational decisions and constraints will affect the actual ΔV placement and magnitude, it was not the intent of this paper to provide an exact (optimal) ΔV location, but rather to provide a reference of feasible transfers and reasonable ΔV locations. Reference designs for each of the orbits are shown in Figures 13 through 17. Additionally, an optimized pre-operational plan will become non-optimal quickly once operational errors are introduced, the schedule for maneuver placement changes, and other operational considerations such as tracking schedules are worked. Figures 13, 14, and 15 show the reverse Earth-Moon departure for each of the example orbits. Each figure is shown in an Earth-Moon rotating frame centered on the Moon. The EML$_2$ Halo and EML$_2$ QuasiHalo departures trajectories are similar to those generated by ATD, see Figures 11 and 12. With the reverse design completed, a forward design was then completed and these trajectories are shown in Figures 16 and 17. These figures are in a solar rotating frame and show all the transfers, and the WFIRST proposed SEL$_2$ orbit.
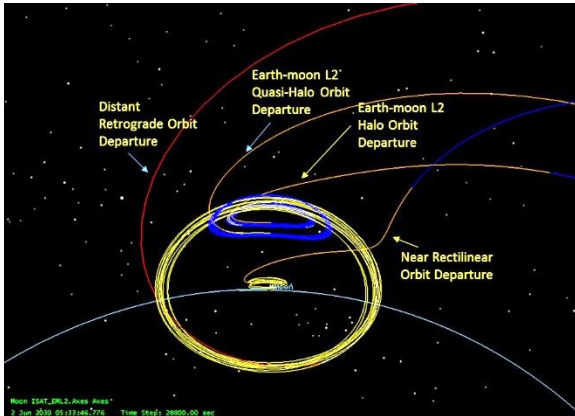
Figure 13. UnStable (Departure) Manifold from all Earth-Moon Examples, Rotating Frame Centered on Moon, along Z-axis
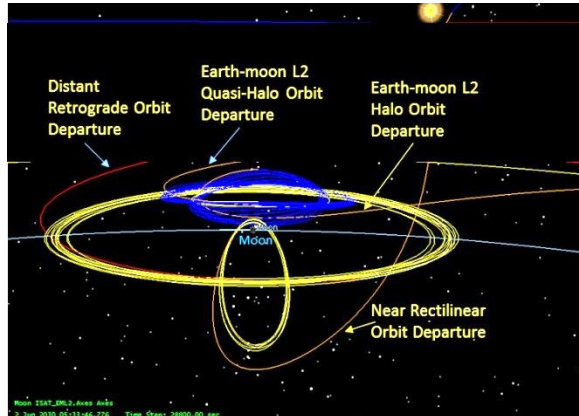

Figure 14. UnStable (Departure) Manifold from all Earth-Moon Examples, Rotating Frame Centered on Moon, along X-axis
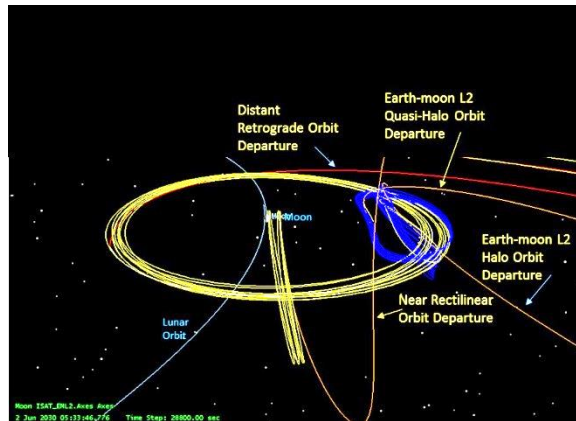

Figure 15. UnStable (Departure) Manifold from all Earth-Moon Examples, Rotating Frame Centered on Moon, along Y-axis
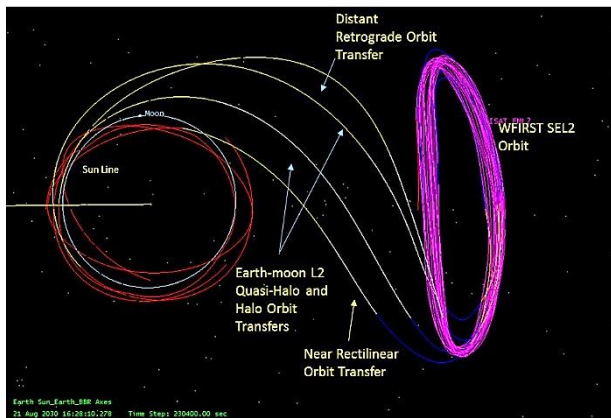

Figure 16. Transfers from SEL$_2$ (WFIRST) to Earth-moon Orbits, Solar Rotating Frame view along Z axis
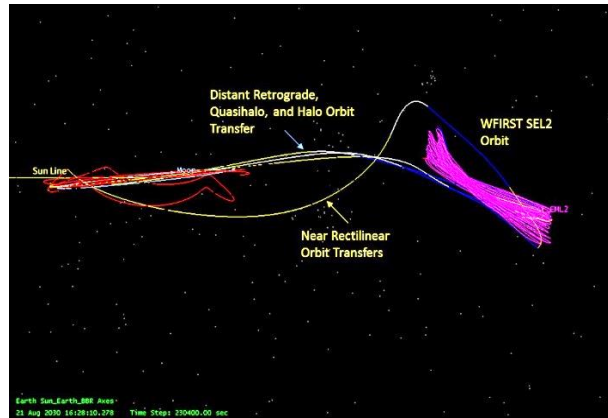

Figure 17. Transfers from SEL$_2$ (WFIRST) to Earth-moon Orbits, Solar Rotating Frame view along Y axis

EML$_2$ Halo, QuasiHalo, DRO and NRHO transfers to SEL$_2$

With the Earth-Moon orbits established from the preceding transfer design and using the aforementioned manifolds, designs where then completed for a transfer from the Earth-Moon region to the SEL$_2$ WFIRST orbit. The departure manifolds from the ATD design were then used to provide the initial maneuver locations in the respective Earth-Moon orbits. These transfers are shown in Figures 18 and 19.
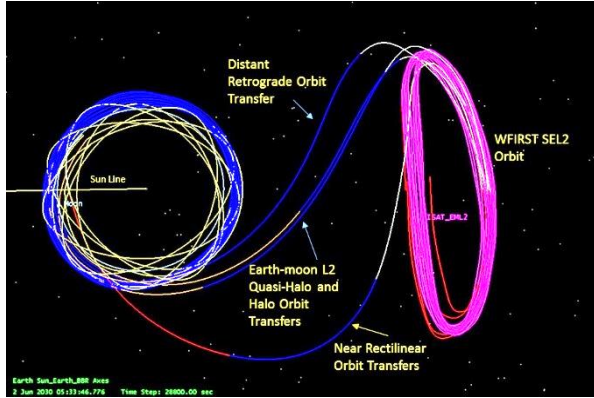

Figure 18. Transfers from Earth-Moon orbits to SEL$_2$ (WFIRST), Solar Rotating Frame view along Z axis
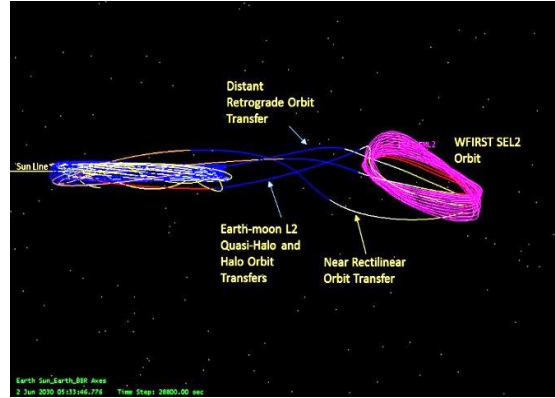
Figure 19. Transfers from Earth-Moon orbits to SEL$_2$ (WFIRST), Solar Rotating Frame view along Y axis

Table 2 provides the basic ΔV and duration information for the reference trajectories used in this analysis. The departure ΔVs for the EML$_2$ QuasiHalo and DRO, labeled as "None, by design", were eliminated by the reverse targeting design process which targeted multiple crossings of the X-Z plane in the SEL$_2$ frame. Note that the transfer duration is the time span between the departure and arrival maneuvers.

Table 2. EML$_2$ and SEL$_2$ (WFIRST) Transfer Options

From Orbit	To Orbit	Departure ΔV (m/s)	Arrival ΔV (m/s)	Transfer Duration (days)
EML$_2$ Halo	SEL$_2$ (WFIRST)	19.5	45.9	134
EML$_2$ Quasi Halo	SEL$_2$ (WFIRST)	29.1	None, by design	94
Lunar DRO	SEL$_2$ (WFIRST)	221.1	35.4	149
NRHO	SEL$_2$ (WFIRST)	16.8	68.3	101
SEL$_2$ (WFIRST)	EML$_2$ Halo	None, by design	38.5	132
SEL$_2$ (WFIRST)	EML$_2$ Quasi Halo	23.5	79.5	127
SEL$_2$ (WFIRST)	Lunar DRO	None, by design	325.8	81
SEL$_2$ (WFIRST)	NRHO	60.2	68.3	142

Observations on Reference Transfer Designs

During the generation of the reference transfer trajectories using the reverse propagation method, it became clear that the orientation of the selected Earth-Moon orbits would have a significant impact on the ΔVs and on operational scenarios to reach the orientation of the WFIRST orbit parameters at the arrival epoch. Using the EML$_2$ Halo orbit as an example, it can be seen in

Figure 19 that the transfer to SEL$_2$ yields an orbit with the SEL$_2$ z-axis component that is out of sync with the desired WFIRST orbit orientation. The difference here is in the SEL$_2$ libration orbit class achieved, either Class-I or II. To accommodate this difference an out-of-plane ΔV was required (and placed) at the same epoch of the nominal initial ΔV required to complete the transfer. This additional ΔV can be quite large, with analysis indicating a required ΔV over 200 m/s.

To eliminate or significantly reduce this required ΔV, the transfer departure date was altered to change the orientation of the EML$_2$ Halo orbit plane with respect to the ecliptic plane yielding a different SEL$_2$ orientation class. The original epoch of the reverse case was in early January 2030. The date needed to be moved between August and October 2030 for the new orbit alignment to eliminate the out-of-plane ΔV component. The reason for this change can be seen in the orientation of the lunar orbit with respect to the ecliptic plane. The lunar orbit is ~5° out of the ecliptic plane. This small plane change and an earlier departure geometry (one with the Sun-Earth-s/c angle < 30°), permits the transfer trajectory to follow a natural motion in the out-of-ecliptic plane. That is, the direction of the departure asymptote is downward with respect to the ecliptic, but the transfer will then exhibit a change with a precession towards the opposite side of the ecliptic plane. The challenge is to fix the departure date so that the final arrival trajectory in the SEL$_2$ region has the correct angle with respect to the ecliptic plane. Figures 20 and 21 show a transfer trajectory design with the date change to align to the SEL$_2$ WFIRST orbit.

The impact of this observation is that the typically quoted ΔVs required to transfer between SEL$_2$ and EM systems are epoch and initial orientation dependent. While use of tools like ATD or other analytical design tools provide a transfer between the chosen orbits, it may not take into account this orientation change, especially if the analysis is performed in a Circular Three Body System with the orbits planar. In addition to the use of a ΔV or date change, a different EML$_2$ Halo class can be used as well to reduce this ΔV.
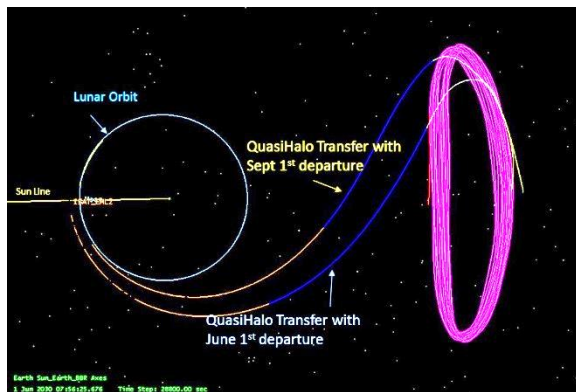

Figure 20. QuasiHalo Transfer Trajectories with different departure dates, viewed from +Z axis in Solar Rotating Frame
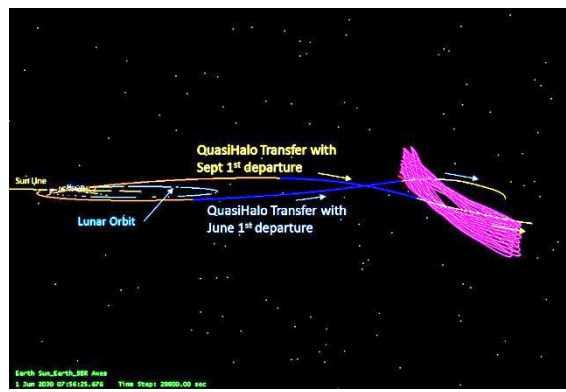
Figure 21. QuasiHalo Transfer Trajectories with different departure dates, viewed from -Y axis in Solar Rotating Frame

NRHO and DRO Orbit Considerations

The NRHO and DRO pose an additional challenge when designing a transfer to or from SEL$_2$. The NRHO orbit, while still an Earth-Moon dynamical systems representation, is more stable and will require a higher ΔV to depart or insert. Additionally, the orbital velocity direction is fixed such that the periapsis velocity is in the same direction of motion as the Moon's orbital velocity so that a departure or insertion is affected by that direction, at periapsis. There is also the effect of the NRHO orbital period of ~ 7 days that limits the coordination between the s/c being at periapsis and

also being at the correct Sun-Earth-Moon angle for the required departure or arrival geometry to minimize the ΔV. And finally, when a maneuver is executed near periapsis in the NRHO, the outgoing direction is not aligned with the ecliptic plane. The maneuver will place the spacecraft on a hyperbolic trajectory with respect to the Moon, so that the outgoing asymptote is towards the south ecliptic pole. The maneuver magnitude needs to be adjusted to permit the natural motion along the manifold and aligned within the ecliptic plane. All of these constraints or requirements feed back into the manifold design generated in ATD. The DRO has similar constraints. The DRO modeled in our analysis was a planar DRO with a low stability index, of ~ 1. This stability means a larger ΔV to depart or insert. Like the NRHO, the DRO orbital velocity direction must line up with the natural outgoing velocity asymptote to provide the minimal ΔV. With a period of ~17 days, timing of the spacecraft location for departure or insertion must be coordinated to when the spacecraft is also at the proper Sun-Earth-Moon angle. The correct combination may not be possible for an extended period so that the transfer may be constrained to a departure or arrival 'window'. Lastly, we did not take into consideration the location of WFIRST in the SEL_2 orbit, i.e we did not consider any rendezvous or approach scenarios. With the transfers from Earth-Moon orbits to SEL_2, the rendezvous/approach problem will also add another requirement or constraint.

The result of these constraints or requirements mean that the timing of a transfer for servicing needs to be planned well in advance. Planning needs to take into consideration the coordination of the departure or insertion with the Sun-Earth-Moon angle, the direction of the outgoing velocity, the out-of-plane components, and the natural motion of the transfer in order to meet the orientation of the SEL_2 orbit plane.

MONTE CARLO TRANSFER ANALYSIS

Having the nominal reference transfers in place for each orbit case, a Monte Carlo analysis was performed to determine the total ΔVs from the effect of navigation errors, maneuver errors, and other related timing sequence influences. Table 3 provides the Monte Carlo errors applied and the location or timing of errors. The Monte Carlo sequence was analyzed for 100 cases given a confidence level near 90%. Errors were placed at critical locations on the transfers but also based on observed operational mission support activities from GSFC supported missions that traversed the Earth-Moon and Sun-Earth regions. These locations were determined based on operational concepts, e.g. the time required for sufficient tracking to converge on a navigation solution and the direction and performance of maneuvers. The time between navigation updates are based on recent GSFC mission support for similar orbits and are based on the ARTEMIS, Deep Space Climate Observatory (DSCOVR), and WMAP missions. These missions all operate in the Earth-Moon and Sun-Earth regions giving an excellent database of operational accuracies.

The Monte Carlo was completed in the following fashion.

1. At an event, such as the SEL_2 departure, apply the nominal maneuver based on the assumed navigation solution.
2. A Gaussian navigation error of 10 km 3-sigma in each position component (uncorrelated) in the SEL_2 region and 1 cm/s 3-sigma in each velocity component (uncorrelated) is applied to the spacecraft state prior to each correction maneuver outside of the EML_2 region. For the correction maneuvers closer to the EML_2 region, the position error is reduced to 1 km 3-sigma. These values are based on a typical orbit determination solution in these regions.
3. The designed correction maneuver is modified to include a 2% hot maneuver error in the direction of the maneuver, which is a typical 3-sigma maneuver error, given that the propulsion system has been calibrated over many maneuvers. This maneuver execution error was a uniform 2% applied only to the maneuver magnitude.

4. Propagate 30 days, to allow time for tracking data measurements to be collected, as is typical for SE libration orbits
5. Take the state at that time from the propagation as the next navigation solution.
6. Calculate the next maneuver to target to the same arrival conditions
7. Repeat processes 2-7 until the arrival condition is achieved.

The covariance used for locations near the SEL$_2$ region was based on WFIRST navigation analysis results which will use the Deep Space Network and the Near Earth Network coverage with several tracking contacts per week. The WFIRST based covariance was used for all navigation errors and maneuvers applied in the SEL$_2$ orbit and during the transfer, both from and to SEL$_2$. The exception to this was the covariance of a navigation solution near the lunar orbit. The covariance for this lunar region is based on the ARTEMIS mission, which was an EML$_2$ orbit as well as a highly elliptical lunar orbit. The 6x6 covariance used only diagonal terms for this analysis and each trajectory will yield different covariance from their respective tracking, measurement biases, and orbit design. The values used in the covariance matrix and maneuver errors are shown in Table 3. Figure 22 gives a representative output of the navigation errors using the diagonal matrix with these input values. As can be seen the 3-sigma position and velocity values are ~ 15 km and 1 cm/s, but the majority of the values are at or below the values in Table 3.

Table 3. Monte Carlo Parameters

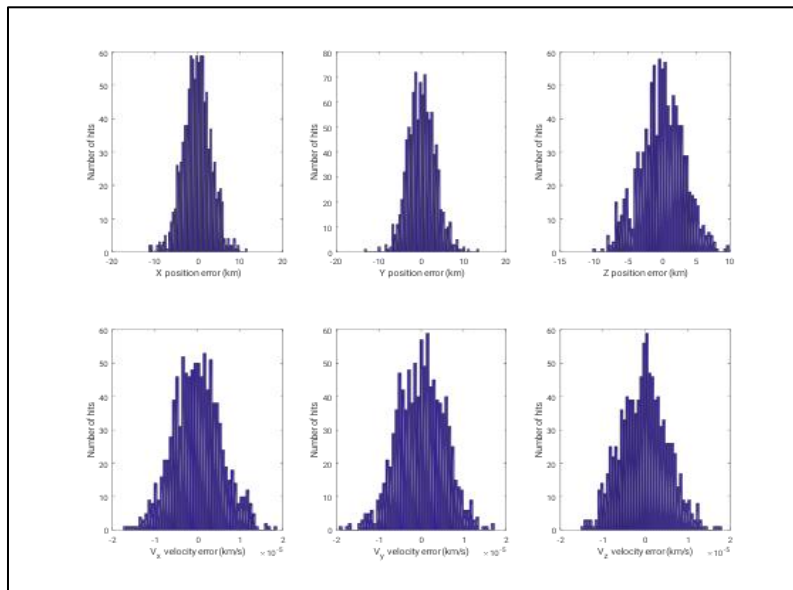| Transfer	3-sigma navigation error	3-sigma maneuver error	Time between navigation errors (days)	Time from navigation solution to maneuver
Near the moon or EML$_2$ orbit	1 km, 0.1 cm/s	2% of magnitude	30	1 day
Near the WFIRST Orbit or in Transfer	10 km, 1 cm/s	2% of magnitude	30	1 day

Figure 22. Sample Navigation Position and Velocity Uncertainties Generated using Covariance

12

DC Maneuver Variable and Goals

On each Monte Carlo case, three transfer maneuvers are incorporated for corrections to the transfer to attain the final targeting state at the related epoch. These maneuvers are composed of the three Cartesian components (e.g. x, y, z in your favorite coordinate frame). The goals of the DC targeter are dependent on the transfer direction. For the transfer from SEL_2 to the Earth-moon orbits, these are simply the position and a velocity component at the epoch of the reference simulation. For example, the insertion state of the EML_2 orbit is chosen. For the transfers to the SEL_2 (WFIRST example), the SEL_2 x-axis velocity along with an SEL_2 x-axis and y-axis position were chosen as the target without a related epoch. As long as the transfer resulted in an SEL_2 orbit that matched the WFIRST configuration, the goals was considered completed. The targeting sequence was setup to have each maneuver with an interval of 30 days target the same goals, providing for the navigation and maneuver errors to be introduced for each target DC iteration.

The effect in the transfer geometry and transfer duration due to navigation and maneuver errors depended on the location in the transfer. For the SEL_2 to Earth-moon transfers, the earlier errors resulted in larger dispersions and thus different trajectories due to the sensitivity while near the SEL_2 orbits. Given the SI associated with the SEL_2 WFIRST reference orbit, it can be seen that the stable and unstable modes are followed. For the transfers initiating in the Earth-moon region and transferring to SEL_2, the initial errors are much less a disturbance. Also, the error associated with the Earth-moon departure orbits is an order of magnitude lower than that at SEL_2. Thus, the transfer are less disturbed.

The Monte Carlo results are shown in Table 4. These results give the overall summary of the ΔVs associated for each of the simulations; four transfers from the SEL_2 WFIRST orbit to the Earth-moon orbits and four transfers from the Earth-moon orbits to the SEL_2 WFIRST orbit.

Table 4. Summary Monte Carlo Results

Transfer Direction	Maximum total *transfer correction* ΔV (m/s)	Maximum change to Insertion maneuver, ΔV (m/s) and Percent
EML_2 Halo to SEL_2	0.28	0.16 (0.3%)
EML_2 QH to SEL_2	1.80	6.4 (24.4%)
DRO to SEL_2	5.30	6.3 (17.8 %)
NRHO to SEL_2	21.80	4.1 (3.1 %)
SEL_2 to EML_2 Halo	0.51	8.0 (25.7 %)
SEL_2 to EML_2 QH	0.13	15.0 (18.9 %)
SEL_2 to DRO	0.08	13.2 (4.0 %)
SEL_2 to NRHO	1.10	1.1 (1.6 %)

Three maneuvers are modeled to correct the perturbed transfer trajectory for each case and are shown in the following figures, 23 through 30. The individual correction maneuvers are shown as the red dashed for the first maneuver which occurs 30 days after the departure, the green at the second maneuver performed 30 days after the first maneuver, and the black for the third maneuver which occurs 30 days after the second maneuver. The magnitude of the combined correction maneuvers remained small, under 1 m/s for all cases simulated except for the DRO and NRHO cases, indicating that the maintenance cost of the transfer based on the assumed navigation and maneuver uncertainties can be easily budgeted within the nominal fuel mass. The effect of the corrections on the insertion maneuver into the SEL2 WFIRST orbit or into the Earth-Moon orbits was dependent on the arrival velocity direction and energy. These results are still under

investigation since the target of the insertion condition included the epoch, position, and a velocity component which in this study was the velocity in the X-axis. These goals were used to constrain the insertion condition so that the insertion maneuver was expected to remain the same, within a small variation. Even with the change to the insertion maneuver, the transfers are still viable within the planned ΔV budget for servicing missions.
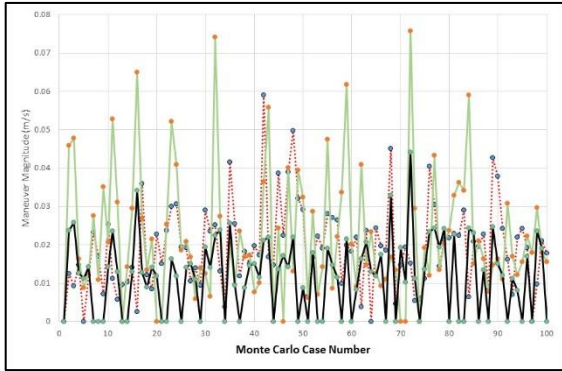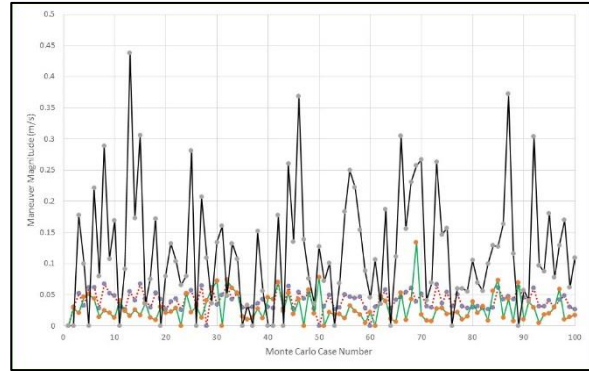

Figure 23. Correction Maneuver Magnitude for SEL₂ to DRO

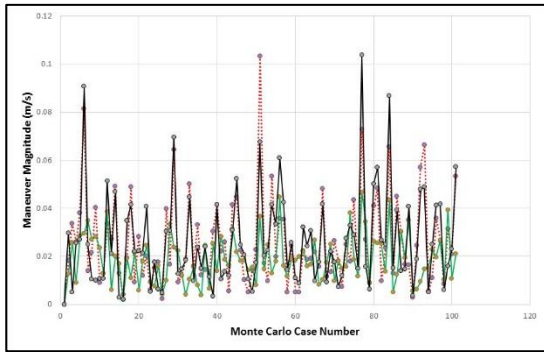**Figure 24. Correction Maneuver Magnitude for SEL₂ to EML₂ Halo**

Figure 25. Correction Maneuver Magnitude for SEL₂ to EML₂ QuasiHalo
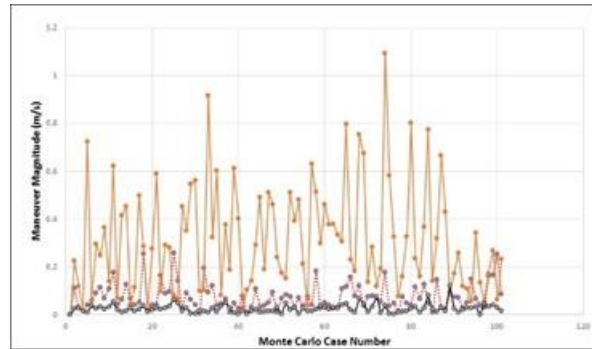

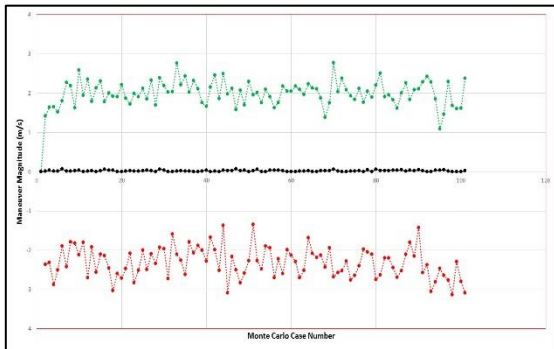**Figure 26. Correction Maneuver Magnitude for SEL₂ to NRHO**

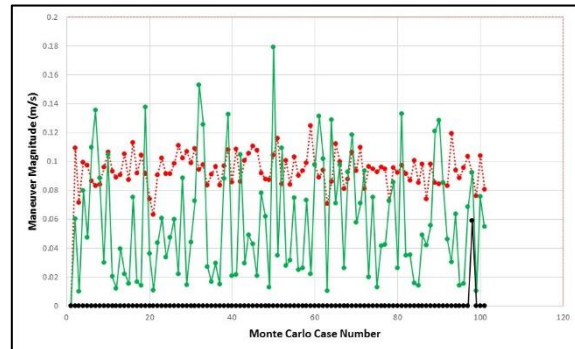**Figure 27. Correction Maneuver Magnitude for DRO to SEL₂**
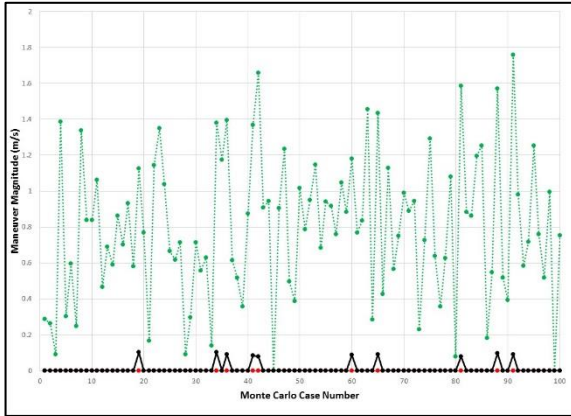

Figure 28. Correction Maneuver Magnitude for EML₂ to SEL₂

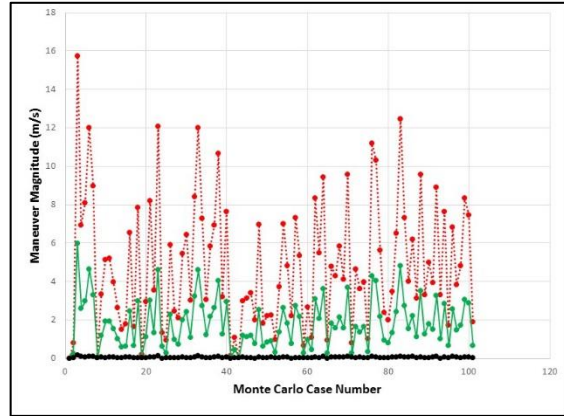**Figure 29. Correction Maneuver Magnitude for EML₂ QuasiHalo to SEL₂**

Figure 30. Correction Maneuver Magnitude for NRHO to SEL₂

Comparison of Transfers from EM orbits to SEL2 QuasiHalo and Lissajous orbits

The aforementioned transfer and insertion ΔV cost were based on the proposed SEL_2 WFIRST QuasiHalo orbit design. A question raised during this analysis was, would the transfer ΔVs and scenarios change drastically if the targeted SEL_2 orbit was a Lissajous orbit rather than the WFIRST QuasiHalo orbit? Therefore a Class-1 Lissajous orbit that meet WFIRST shadow and angle requirements was generated for a comparison. This orbit is shown in Figures 31 and 32. The deterministic maneuvers to transfer to and enter into the Lissajous are based on the previous EM to SEL_2 analysis, but will require additional ΔVs to attain the Lissajous SEL_2 Z-amplitude and to match the Lissajous velocity conditions via the insertion maneuver. In general, the increase in the ΔVs was on the order of 200 m/s with the majority of the ΔV in the out-of-ecliptic-plane direction. The modification of the aforementioned transfers to achieve Lissajous insertion targeted the conditions at the rotating x-axis crossing (y axis = 0) at which point the insertion maneuver was performed. The out-of-plane maneuvers were first distributed equally beginning at the departure maneuver and then also applied to the transfer maneuvers at the 30-day intervals. There are limitations on the magnitude of the departure out-of-plane maneuver as that can result in an orbit (energy and direction) that does not transfer towards SEL_2, but remains within the Cislunar space. The entirety of the out-of-plane maneuvers were used to shape the trajectory so that the SEL2 x-axis crossing occurred at the maximum negative SEL_2 z-axis. The insertion maneuver occurred at this location.

Table 5 compares the ΔVs from the above EM orbit transfers to the QuasiHalo to the Lissajous orbit. As can be seen the largest difference is the out-of-plane components. These ΔVs may be minimized by the selection of an alternate departure date which would provide an improved alignment of the departure asymptote (departure from the lunar orbit plane) onto the transfer manifold required to attain a larger Lissajous SEL_2 Z-amplitude. Analysis to study this epoch alignment effect was not performed in this investigation. Table 5 provides an overview of the ΔV differences. The information in the table shows the departure, insertion, and total ΔVs for the QuasiHalo and the departure, additional transfer, insertion, and total ΔVs for the Lissajous. The last column highlights the ΔV increase (Lissajous minus QuasiHalo) and the out-of-plane ΔV required to match the Lissjaous orientation and amplitude. Based on altering the preceding design (assuming the same departure date and orientation in the EM orbit), the increase in the ΔV is dependent on the initial EM orbit. This is an obvious observation but the magnitude of the increase is quite large, ranging from twice the QuasiHalo ΔV magnitude to almost 15 times, with the majority of the ΔV

in the out-of-plane direction. This ΔV is still reasonable when compared to lunar and planetary mission designs but may be minimized by selecting alternate EM orbit designs to align the transfer trajectory with the Lissajous arrival condition.
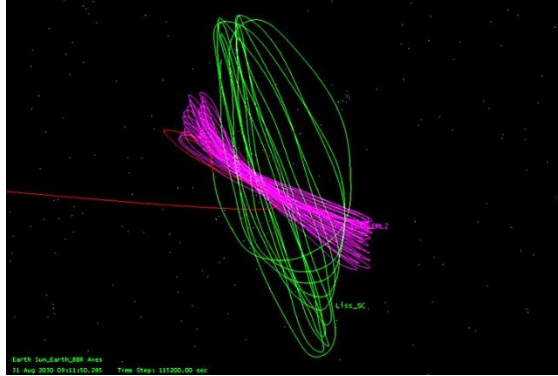

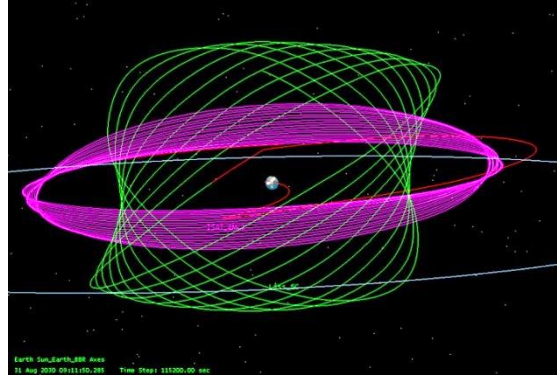**Figure 31. QuasiHalo and Lissajous Orbits viewed from -Y axis in SEL₂ Solar Rotating Frame**

Figure 32. QuasiHalo and Lissajous Orbits viewed from +x axis in SEL₂ Solar Rotating Frame

Table 5. Comparison of SEL2 QuasiHalo and Lissajous transfer ΔV magnitudes

Departure Location	ΔVs (m/s) to QuasiHalo Departure : Insertion : **Total**	ΔVs (m/s) to Lissajous Departure : Transfer : Insertion : **Total**	ΔV (m/s) increase, Departure + Transfer, and Out-of-Plane
EML₂ Halo	19.5 : 45.9 : **65.4**	23.2 : 236.0 : 201.1 : **460.3**	239.7 : 230.0
EML₂ QuasiHalo	29.1 : 0.0 : **29.1**	200.1 : 120.2 : 130.5 : **450.8**	291.2 : 320.2
DRO	221.1 : 35.4 : **256.5**	221.1 : 200.6 : 96.2 : **517.9**	165.2 : 200.0
NRHO	16.8 : 68.3 : **85.1**	16.8 : 111.0 : 45.9 : **173.7**	42.7 : 110.0

Differences in the transfer trajectories for the EML₂ case can be seen in Figure 33 and 34. These transfers are based on the same EML₂ Halo orbit used in the previous analysis. The transfers from the other Earth-moon locations are similar in design and show the increase in the transfer SEL₂ Z-amplitude in order to attain the Lissajous orbit dimensions and the orientation of the orbit for the class type. The updated transfers attained the required x-axis and z-axis values at the x-z plane crossing (y-axis = 0).
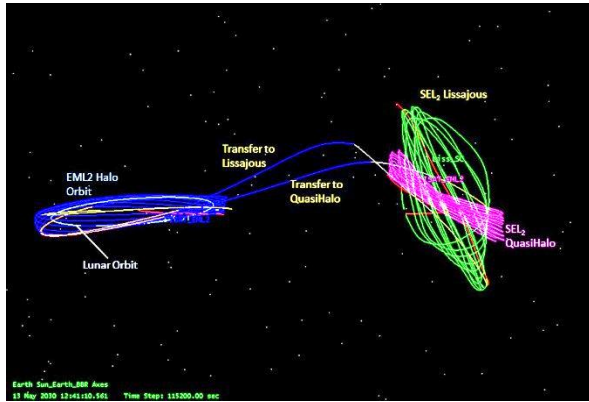
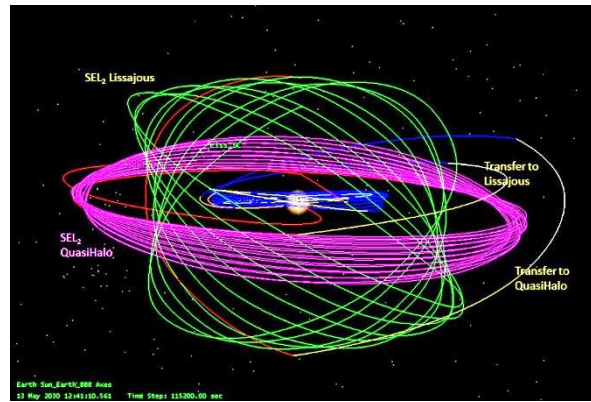**Figure 33. EML₂ Halo Transfers to QuasiHalo and Lissajous Orbits viewed from -Y axis in Solar Rotating Frame**

Figure 34. EML₂ Halo Transfers to QuasiHalo and Lissajous Orbits viewed from +x axis in Solar Rotating Frame

SUMMARY

An analysis of transfers between the Earth-Moon region using the EML$_2$ Halo and QuasiHalo orbits, NRHO, and a DRO with a reference orbit, WFIRST at SEL$_2$, was completed. These particular orbits are candidates for possible servicing locations for future science missions at SEL$_2$ and assembly for missions to be placed at SEL$_2$. In completing this analysis, it was found that the simplified assumptions of transferring between these orbits can be used as an initial guideline for designs, but cannot be used to determine the proposed ΔV budget. A detailed investigation must be made that includes the orbit geometry, the orbit departure and arrival conditions, and the timing. The orientation of the orbits (e.g. class I or II types) will make a difference in the allowable timeframe of transfers as well. It was found that the departure periods are extremely limited, depending on the orbit class and the synchronization of the transfer to meet the arrival goals. Timing in the departure from the Earth-Moon orbits is critical as the correct alignment in the Moon's orbit plane, e.g. below or above the ecliptic plane, is necessary to align the trajectory that enters the SEL$_2$ orbit. While this paper did not investigate rendezvous between WFIRST and the servicing vehicle, it is important to note that rendezvous may introduce a significant constraint to the number of transfer trajectories and require substantially increased ΔV. The purpose of the paper was to investigate the viability of the transfers and the impact of navigation and maneuver uncertainties.

The calculated ΔVs from this study, while larger that the typically referenced EML$_2$ - SEL$_2$ transfers using CRTBP profiles and dynamics, are still within the realm of a minimal ΔV cost. The transfer trajectory correction ΔVs, considering the departure, insertion, and navigation and maneuver uncertainties, are near single m/s level with the exception of the NRHO case. The Monte Carlo results used operational data to guide the navigation and maneuver uncertainties, and indicated that the maneuvers and total ΔV cost are within the typical ΔV budget for missions to the Sun-Earth libration orbits. The ΔVs found in this study are assumed to be feasible designs, and the 'optimal' ΔVs can be found for individual cases by making changes to the departure and arrival epochs.

CONCLUSION

Based on the Earth-Moon and SEL$_2$ orbit types studied and the related orbital constraints or requirements used in this analysis, results indicate that the timing of servicing transfers needs to be

planned well in advance. This planning must take into consideration the synchronization of the departure or insertion location within the servicing orbit with the Sun-Earth-moon angle at departure or arrival, the direction of the outgoing velocity, out-of-plane components of the Earth-Moon or SEL$_2$ orbit, and the natural motion of the transfer to meet the orientation of the SEL$_2$ orbit plane. The combination of orbit orientation such as Northern or Southern EML$_2$ Halos for example, may also constrain the natural manifold selection to occur at a given epoch that is related to lunar orbit plane orientation at departure or arrival. The ΔV budget should also consider the effects of navigation and maneuver uncertainties since the initial EML$_2$ and SEL$_2$ transfer segments are in a chaotic environment and sensitive to small perturbations. The ΔV budget for correction maneuvers along the transfer remained manageable at a level of single m/s.

ACKNOWLEDGEMENTS

REFERENCES

1. Website,https://spacenews.com/scientists-and-engineers-push-for-servicing-and-assembly-of-future-space-observatories/
2. Website, "in-Space Assembled Telescope" Study, (iSAT)https://www.scientificamerican.com/article/finding-alien-life-may-require-giant-telescopes-built-in-orbit/, 2018
3. K. Howell, D. Mains, B. Barden, " Transfer Trajectories from Earth Parking Orbits to Sun Earth Halo Orbits", AIAA 94-160, AAS/AIAA SpaceFlight Mechanics Meeting, Cocoa Beach, FL, 1994
4. K. Howell, M. Kakoi, "Transfers between the Earth-Moon and Sun-Earth Systems using Manifolds and Transit Orbits", Acta Astronautica, 59 (2006) 367-380, May 12, 2006
5. D. Folta, et al, "Servicing and Deployment of National Resources in Sun-Earth Libration Point Orbits", 53rd International Astronautical Congress, World Space Congress, Houston, TX, Oct 10-19, 2002
6. D. Folta, F. Vaughn, A Survey Of Earth-Moon Libration Orbits: Stationkeeping Strategies And Intra-Orbit Transfers, AAS/AIAA Astrodynamics Specialist Conference, Lake Tahoe, California, August 7-11, 2005
7. D. Folta, M. Woodard, T. Sweetser, S. Broschart, and D. Cosgrove, "Design and Implementation of the ARTEMIS Lunar Transfer Using Multi-body Dynamics", AAS/AIAA Astrodynamics Specialist Conference held August 1-4 2011, Girdwood, Alaska.
8. Davis, D.C., Philips, S.M., Howell, K.C., Vutukuri, S., and McCarthy, B.P., "Stationkeeping and Transfer Trajectory Design for Spacecraft in Cislunar Space," AAS/AIAA Astrodynamics Specialist Conference, Columbia River Gorge, Stevenson, Washington, August 21 - 24, 2017.
9. David C. Folta, Cassandra M. Webster, Natasha Bosanac, Andrew Cox, Davide Guzzetti, and Kathleen C. Howell, Trajectory Design Tools for Libration and Cis-Lunar Environments", 6th International Conference on Astrodynamics Tools and Techniques (ICATT), Darmstadt, Germany, December 2015
10. S. Leete, "Design for On-Orbit Spacecraft Servicing", Proceedings of the 2001 Core Technologies for Space Systems Conference, Colorado Springs, CO, 11/28-30, 2001.
11. N. Bosanac, C. M. Webster, K. Howell and D. C. Folta, "Trajectory Design and Station-Keeping Analysis for the Wide Field Infrared Survey Telescope Mission", in AAS/AIAA Astrodynamics Specialist Conference, 2017.
12. C. Webster, D. Folta, "IWSCFF 17-74: Understanding the Sun-Earth Libration Point Orbit Formation Flying Challenges for WFIRST and Starshade", 9th International Workshop on Satellite Constellations and Formation Flying, June 2017, Boulder, Co.